Geophysical Research Letters

RESEARCH LETTER
10.1029/2021GL093045

Revisiting AMOC Transport Estimates From Observations and Models

Gokhan Danabasoglu[1,2], Frederic S. Castruccio[1,2], R. Justin Small[1,2], Robert Tomas[1], Eleanor Frajka-Williams[3], and Matthias Lankhorst[4]

[1]Climate and Global Dynamics Laboratory, National Center for Atmospheric Research, Boulder, CO, USA, [2]International Laboratory for High-Resolution Earth System Prediction, Texas A&M University, College Station, TX, USA, [3]Ocean and Earth Science, University of Southampton, Southampton, UK, [4]Scripps Institution of Oceanography, University of California San Diego, La Jolla, CA, USA

Key Points:

- Assumptions used in observational Meridional Overturning Variability Experiment (MOVE) and RAPID transport estimates are revisited in eddying model simulations
- Results reinforce the need for proper treatments of reference depths and velocities in geostrophic calculations in observations and models
- Simulated variability and trends at MOVE and RAPID locations are mostly consistent between the two sites, particularly on long time scales

Supporting Information:

Supporting Information may be found in the online version of this article.

Correspondence to:

G. Danabasoglu,
gokhan@ucar.edu

Citation:

Danabasoglu, G., Castruccio, F. S., Small, R. J., Tomas, R., Frajka-Williams, E., & Lankhorst, M. (2021). Revisiting AMOC transport estimates from observations and models. *Geophysical Research Letters*, *48*, e2021GL093045. https://doi.org/10.1029/2021GL093045

Received 18 FEB 2021
Accepted 6 MAY 2021

Abstract Reference level assumptions used to calculate the Atlantic meridional overturning circulation transports at the RAPID and Meridional Overturning Variability Experiment (MOVE) observing arrays are revisited in an eddying ocean model. Observational transport calculation methods are complemented by several alternative approaches. At RAPID, the model transports from the observational method and the model truth (based on the actual model velocities) agree well in their mean and variability. There are substantial differences among the transport estimates obtained with various methods at the MOVE site. These differences result from relatively large and time-varying reference velocities at depth in the model, not supporting a level-of-no-motion. The methods that account for these reference velocities properly at MOVE produce transports that are in good agreement with the model truth. In contrast with the observational estimates, the model transport trends at MOVE and RAPID largely agree with each other on pentadal to multi-decadal time scales.

Plain Language Summary Ocean transport arrays measure the mean and variability of ocean circulation. Due to technical, logistical, and financial constraints, these arrays do not measure ocean currents directly, but rather rely on a limited set of measurements leveraged by fundamental governing equations. Two observational arrays in the subtropical North Atlantic use these equations subject to some assumptions. In this study, a high-resolution ocean model is employed to test these assumptions by estimating ocean transports in the model according to the methods applied at the two arrays. The model solutions do not support these assumptions at one of the sites. Nevertheless, there is an agreement in transport trends at both sites in the model, in contrast with the observational estimates. Proper determination of reference velocities in observations is important to advance understanding of basin-wide circulation and its changes in the Atlantic Ocean.

1. Introduction

The Atlantic Meridional Overturning Circulation (AMOC) is important to climate variability and change, especially through its associated meridional heat, freshwater, and carbon transports (see Buckley & Marshall, 2016; Sutton et al., 2018, and Zhang et al., 2019 for recent reviews of the current state of research on AMOC and its climate impacts). For a long time, measurements have been made of some key parts of AMOC, such as the Deep Western Boundary Current (DWBC at Line W at 39°N; Toole et al., 2011, 2017) and the Florida Current (Larsen & Sanford, 1985; Meinen et al., 2010; Sanford, 1982), and from intermittent hydrographic sections (e.g., Bryden et al., 2005). Over the last two decades or so, observational efforts gained significant momentum with several trans-basin and western boundary arrays in place, aiming to measure AMOC more comprehensively and continuously. These efforts include the Meridional Overturning Variability Experiment array at 16°N since 2000 (MOVE; Send et al., 2011); the RAPID Array at 26.5°N since 2004 (Cunningham et al., 2007); the South Atlantic MOC Basin-wide Array at 34.5°S since 2009 (SAMBA; Meinen et al., 2018); and the Overturning in the Subpolar North Atlantic Program array at 57°N since 2014 (OSNAP; Lozier et al., 2019). Due to technical, logistical, and financial limitations, the observational estimates are typically done using a small set of instruments and applying fundamental physical assumptions such as geostrophic dynamics. However, the methodologies used for each program differ, as a particular method may work better at a particular location, and for the limitations just indicated. Comprehensive

reviews of the observational programs in the Atlantic Basin are provided in Bower et al. (2019), Frajka-Williams et al. (2019), and McCarthy et al. (2020).

Each of these observational campaigns requires significant planning prior to its deployment to evaluate observational approaches and assumptions that may also include performing Observing System Simulation Experiments (e.g., Hirschi et al., 2003; Kanzow et al., 2006; Li et al., 2017; Perez et al., 2011). Among these programs, arguably, the RAPID array has attracted the most attention due to its relatively long, trans-basin AMOC transport record, with many studies using its results, but also scrutinizing its underlying assumptions. For example, Roberts et al. (2013) find good agreement between the observed and simulated deep AMOC when they calculate model transports using the same assumptions as in observations. They also report a sensitivity of the observed profile of AMOC to the choice of a reference depth. Stepanov et al. (2016) report sensitivities of deep volume and heat transports for this site to the details of both geostrophic and ageostrophic components. In a recent study, Sinha et al. (2018) perform a very detailed and comprehensive evaluation of all RAPID approximations, finding that the RAPID method underestimates the mean AMOC by about 1.5 Sv (1 Sv = 10^6 m^3 s^{-1}), but captures variability with high accuracy, both in comparison to a high-resolution ocean model simulation. For the MOVE site, the assumption of monitoring only the southward DWBC–associated with the North Atlantic Deep Water (NADW)—flow to infer AMOC variability is supported by numerical simulations (Kanzow et al., 2008). In addition, the assumption that there is a level-of-no-motion at depth on long timescales (Send et al., 2011) seems to be supported, at least for the period covering the last two decades, by a recent study based on data from the Gravity Recovery and Climate Experiment mission (GRACE; Koelling et al., 2020).

The time series from MOVE and RAPID—the two sites with the longest records—show both rich variabilities on inter-annual to decadal time scales and decadal-scale trends (e.g., Roberts et al., 2013, 2014; Send et al., 2011; Smeed et al., 2014, 2018). However, because the data sets are relatively short, it remains largely uncertain whether any identified short-term trends are part of a longer-term trend or just represent intrinsic decadal (or longer) variability. Contemporaneous data from these two sites—as well as from other sites as they become available—are also useful to evaluate meridional consistency (or coherency) of AMOC properties, including variability and trends. In a detailed comparison of the RAPID and MOVE data sets, Frajka-Williams et al. (2018; hereafter FW18) show that the respective estimation methods lead to opposing trends in AMOC during 2004–2015 at the two sites: a weakening at RAPID and a strengthening at MOVE. In particular, the study finds that although the baroclinic part (geostrophic shear) is similar between MOVE and RAPID, the total AMOC differs, implying that how the barotropic part is accounted for results in these trend differences.

Comparing model simulations of AMOC characteristics with those from available observations is clearly essential for assessing the quality of our models and advancing their fidelity (e.g., Danabasoglu et al., 2018). It is important that such model—observations comparisons use the same methods as applied in observations to provide apples-to-apples comparisons. In this study, considering both the RAPID and MOVE sites together, we revisit and re-evaluate the underlying assumptions used to calculate their respective transports in comparison to transports from an eddying ocean hindcast simulation where transports obtained using the same observational methods—as well as a few alternative approaches—can be directly compared against model *truth*. Particular attention is paid to the details and impacts of reference levels and associated reference velocities. In addition, the consistency of simulated trends at the MOVE and RAPID sites are investigated on pentadal and longer time scales with a focus on the 2004–2015 period for which conflicting trends from observations were reported in FW18.

2. Observations, Model, and Methods

2.1. Meridional Overturning Variability Experiment

The MOVE array has measured the southward transport associated with the NADW below 1,200-m depth at 16°N between Guadeloupe to the west (60.5°W) and the Mid-Atlantic Ridge (MAR) to the east (51.5°W) since January 2000 (Send et al., 2011; see Figure 1b and Text S1 here). As such, it is assumed that the NADW is mostly confined to this region, and any transport to the east of the MAR is neglected. The transport is computed as the sum of a boundary component from direct current meter measurements on the

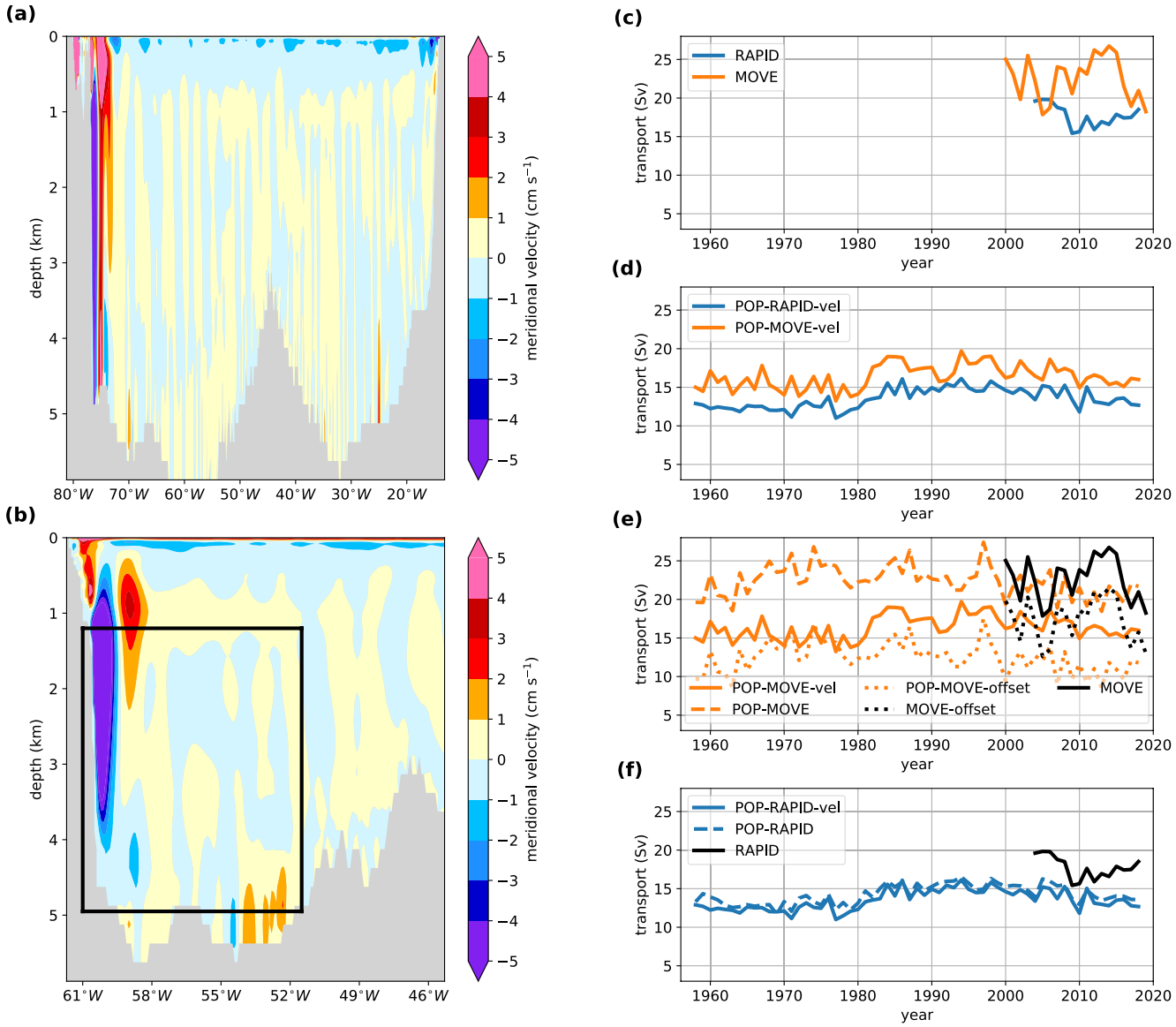

Figure 1. The 1958–2018-mean meridional velocity from FOSI at (a) the RAPID 26.5°N and (b) MOVE 16°N sites with positive and negative contours showing northward and southward flows, respectively, in cm s^{-1}. In (b), the MOVE domain covered by the observations is shown by the black rectangle. Annual-mean time series of (c) the MOVE and RAPID observational transport estimates; (d) MOVE and RAPID transports calculated using the model meridional velocity from FOSI; (e) transports for the MOVE site from FOSI calculated using the POP-MOVE-vel, POP-MOVE, and POP-MOVE-offset methods; and (f) transports for the RAPID site from FOSI calculated using the POP-RAPID-vel and POP-RAPID methods. For ease of comparison, the southward transports at MOVE are shown as positive transports in (c–e). In (e and f), the solid black lines denote the respective observational transports.

western side and an internal component using dynamic height profiles referenced to zero flow at 4,950 m. This depth represents an approximate boundary between the NADW and the northward flowing Antarctic Bottom Water (AABW). Due to the uncertainties associated with the reference level velocities (external or barotropic component), the MOVE array is more suited for measuring variability.

2.2. RAPID

The RAPID array estimates the total AMOC transport across the entire Atlantic Basin at 26.5°N since April 2004 (Text S1). It includes four components: western boundary wedge (WBW), Florida Current, interior or mid-ocean, and the wind-driven, near-surface Ekman part (e.g., Cunningham et al., 2007; McCarthy et al., 2015). The WBW flow is directly measured by current meters. The Ekman flow is estimated using

reanalysis products. The Florida Current is measured electromagnetically via a submarine cable (Larsen & Sanford, 1985; Meinen et al., 2010; Sanford, 1982). As with MOVE, RAPID uses an end-point geostrophy approximation to obtain mid-ocean transport. A bottom-up integration with a level-of-no-motion at 4,820 dbar is used, but to counter the possible error this creates, a mass-compensation term of ∼10 Sv is added, essentially accounting for the barotropic component. Specifically, a longitude-independent, but time-varying barotropic velocity is added to the mid-ocean geostrophic velocity to ensure zero net flow through the section.

2.3. Model and Simulation

An eddying, Forced Ocean-Sea-Ice (FOSI) hindcast simulation with a nominal 0.1° horizontal resolution (see Chassignet et al., 2020 for a summary of the model configuration) is analyzed. This configuration uses the Community Earth System Model version 2 (CESM2; Danabasoglu et al., 2020) framework. The simulation is forced with the adjusted Japanese Reanalysis data sets (JRA55-do; Tsujino et al., 2018) for the 1958–2018 period and has been performed by the International Laboratory for High-Resolution Earth System Prediction (iHESP; Chang et al., 2020). The 1958–2018 forcing period is cyclically repeated multiple times to reduce model transients and drifts. The results from the third repeat cycle are used in this study. The solutions from a corresponding nominal 1° resolution version of the model are qualitatively very similar. The CESM2 ocean component is the Parallel Ocean Program version 2 (Danabasoglu et al., 2012; Smith et al., 2010), and *POP* prefix will be used to denote the model results.

2.4. Methods

Several methods are considered to calculate transports for the RAPID and MOVE sites from model simulations as detailed in the Supplementary Information (Text S1 and Table S1). The observational data are denoted as *RAPID* and *MOVE*, respectively. The model transports estimated using the equivalent respective observational methods are denoted as *POP-RAPID* and *POP-MOVE*. These calculations use the Meridional ovErTurning ciRculation diagnostIC (METRIC) package which enables consistent calculations of AMOC estimates at the MOVE and RAPID sections from observations and models (Text S1). The transports based on the model meridional velocities integrated across the respective arrays—the model *truth*—are labeled as POP-*RAPID-vel* and *POP-MOVE-vel*. The model-computed overturning circulation across the entire Atlantic, labeled as *POP-MOC*, is used to assess how representative the MOVE transports are for the entire 16°N section. The transports shown as *POP-MOVE-ref* employ the time-varying model meridional velocities at 4,950 m as reference velocities, rather than assuming a level-of-no-motion. Finally, *POP-MOVE-td* computes the geostrophic velocities starting from the surface down and using the sea surface height to infer the time-varying barotropic term needed to calculate absolute geostrophic velocities.

Some of the MOVE data sets from observations incorporate an adjustment of the internal component that removes the temporal mean of the velocity at 1,200 m. This time-invariant correction is applied as a barotropic correction to the internal component only. Essentially, this approach maintains the variability present in the deep reference level method but shifts the mean to be more consistent with the (better-defined) water mass boundary between the Antarctic Intermediate Water and NADW at 1,200 m. The observational and model transports computed this way are denoted as *MOVE-offset* and *POP-MOVE-offset*, respectively.

3. Results

Time-mean meridional velocity distributions from FOSI for the RAPID and MOVE sites are presented in Figures 1a and 1b, respectively, showing a strong southward flow at the western boundary below ∼500-m depth, associated with the NADW, and an adjacent northward flow in both. The latter is stronger and penetrates deeper at RAPID than at MOVE. At both sites, the interior flow is relatively weak, alternating between northward and southward and mostly remaining <0.01 m s^{-1}. The northward flowing AABW is clearly evident at the MOVE site below 4,000-m depth and to the west of MAR with its mean velocity reaching 0.02 m s^{-1}.

The remaining panels of Figure 1 show the time series of various annual-mean transport estimates for MOVE and RAPID. Although there are trends on interannual-to-pentadal time scales in observations, it is not obvious that such trends are distinct from longer-term variability when viewed from a (multi-)decadal perspective (Figure 1c). As discussed in FW18, there are significant differences in short-term trends in the two observational estimates. Indeed, the figure shows opposite trends in the observations toward the end of the records as well—a period not considered in FW18: while there is a sharp decline at MOVE, the transport at RAPID has a gradual increase. As discussed earlier, such discrepancies in the observations have been attributed to various issues with the calculation of the barotropic component (FW18; also see below).

The model transports obtained using the meridional velocities—the model *truth*—are given in Figure 1d for MOVE and RAPID for the entire FOSI simulation period. In general, the two time series show agreement in their low-frequency variability, with both transports remaining steady until the late-1970s, increasing until about the mid-1990s, and then gradually decreasing, consistent with the findings of Danabasoglu et al. (2016). The mean transports are 16.4 $\pm$ 1.5 and 13.5 $\pm$ 1.3 Sv for the period 1958–2018 for POP-MOVE-vel and POP-RAPID-vel, respectively, with the range showing one standard deviation. Interestingly, almost identical respective mean transports are obtained in the model for both sites during the period of the observational records. The model transports are lower than the observational estimates of 22.6 $\pm$ 2.8 Sv for MOVE and 17.7 $\pm$ 1.4 Sv for RAPID based on the annual-mean data during their respective periods. As shown and discussed in Danabasoglu et al. (2014, 2016), Chassignet et al. (2020), and Tsujino et al. (2020) for RAPID, AMOC transports in FOSI simulations are usually weaker than in observations with AMOC magnitude depending on forcing, model parameterizations and resolution, and strength of surface salinity restoring. For example, in contrast with the FOSI simulation analyzed here, a previous simulation with CESM1 which was forced with an older atmospheric data set shows stronger AMOC in good agreement with the RAPID observations (Danabasoglu et al., 2014, 2016). The model standard deviations given above for POP-RAPID-vel and POP-MOVE-vel are consistent with the higher observed variability at MOVE than at RAPID reported in FW18. A likely reason for this higher variability at MOVE is that there is no compensating transport applied at this site because it is not a full-basin array. At RAPID, both in observations (Figure 12 of FW18) and FOSI (Figure S1), variability of the compensating transport is negatively correlated with that of the interior transport, significantly reducing the variability of the total transport, especially in the presence of relatively weak interannual to decadal variability in the Florida Current, Ekman, and WBW transports. The simultaneous correlation coefficients between POP-MOVE-vel and POP-RAPID-vel are computed as +0.72 and +0.56 for the 1958–2018 and 2004–2018 periods, respectively, based on the annual-mean time series. These positive correlation coefficients are in stark contrast with a correlation coefficient of −0.47 between the two observational estimates during their common period.

Figures 1e and 1f present the transport estimates from FOSI using the respective, equivalent observational methods in comparison to the model truth and observational estimates. There are significant differences among the model estimates for MOVE which also differ from the observational estimates. Application of an adjustment (or offset) does not impact variability but reduces the transport in both observations and model by 5 and 10 Sv, respectively. In contrast, the RAPID observational method agrees remarkably well with the model truth at this site. As indicated above, in comparison to observations, the model transports at RAPID are weaker and the model does not seem to capture the gradual increase at the end of the record. The reason for this latter discrepancy is under further investigation.

Transport estimates for MOVE from all the methods considered here from FOSI are summarized in Figure 2a, clearly showing large differences in the estimates. The 1958–2018 mean transports range from 12.5 and 12.9 Sv with POP-MOVE-offset and POP-MOVE-ref, respectively, to 22.4 Sv with POP-MOVE (Table S2). The range of variability based on the standard deviations from the annual means is 1.5 Sv (POP-MOVE-vel) to 2.0 Sv (POP-MOVE and POP-MOVE-offset). With respective correlation coefficients of 0.87 and 0.94, POP-MOVE-ref and POP-MOVE-td—the two methods that employ time-varying reference velocities—are the closest to the model truth (POP-MOVE-vel). In contrast, the two observational-based methods (POP-MOVE and POP-MOVE-offset) that use a time-independent, that is, zero, reference velocity have the lowest correlations with the model truth.

To assess how representative the MOVE transports are for the entire 16°N section in FOSI, the black line in Figure 2a shows the trans-basin AMOC transport. Both the mean transport and its variability for

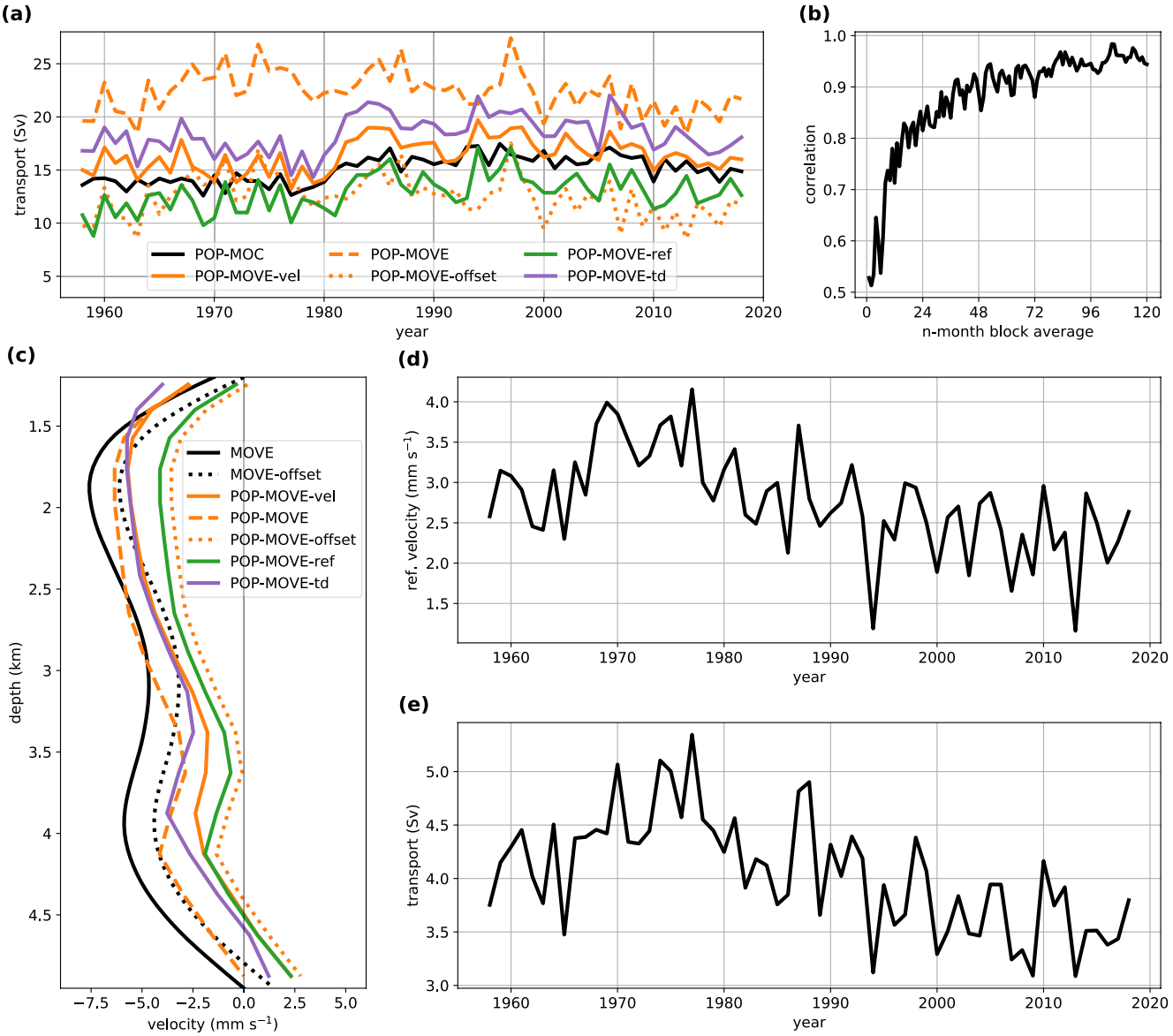

Figure 2. (a) Annual-mean time series of transport estimates at MOVE from FOSI obtained using various methods as summarized in Section 2.4 and Table S1. The orange lines are the same as in Figure 1e. The southward transports at MOVE are shown as positive transports. (b) Correlation coefficient between the model AMOC strength (computed across the full basin width, POP-MOC) and the transport estimated using the POP meridional velocity across the MOVE section (POP-MOVE-vel) as a function of the block-averaging length used to low-pass filter each time series. (c) The 2000–2018-mean and zonal-mean meridional velocity profiles for the internal component of the MOVE transport estimate. The black solid line is the MOVE observational estimate computed via geostrophy referenced to zero flow at 4,950 m. The black dotted line is the adjusted MOVE observational estimate where a time-invariant barotropic correction is added to the estimate to ensure zero flow at 1,200-m depth. The remaining lines are from FOSI, showing profiles for all the considered methods. Time series of (d) annual- and zonal-mean reference velocity at 4,950 m and (e) annual-mean AABW transport for the MOVE section from FOSI defined as the northward flow below 4,500 m.

POP-MOVE-vel are higher than those of the trans-basin AMOC (POP-MOC). Indeed, POP-MOC has the lowest variability among the model transport estimates (Table S2), likely due to compensating flows and reduction in variability when integrated across the basin as discussed for RAPID above. POP-MOVE-vel and POP-MOC time series are correlated at ~0.71. More generally, correlation coefficients between these two transport estimates as a function of the block-averaging length used to low-pass filter each time series are given in Figure 2b. The figure shows that the MOVE estimates are good approximations for the total trans-basin transport particularly on pentadal and longer time scales with correlation coefficients of >0.9. Based on a two-sided Student's t-test and considering reduced effective degrees of freedom with

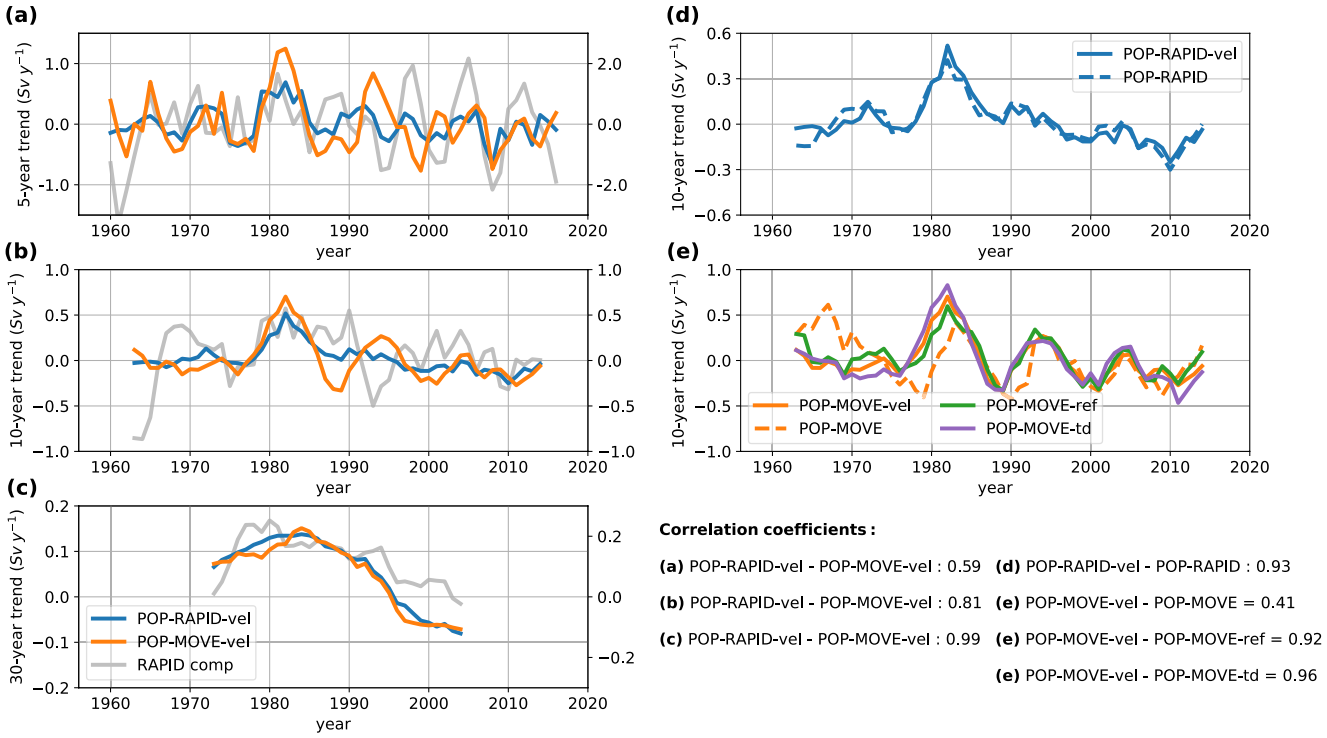

Figure 3. Time series of the (a) 5-year, (b) 10-year, and (c) 30-year trends for MOVE and RAPID obtained with the POP-RAPID-vel and POP-MOVE-vel methods. In these panels, the light gray lines show the trend time series for the compensating transport at RAPID with their scales on the right vertical axis. Time series of 10-year trends for (d) RAPID and (e) MOVE from the transport methods considered. All the time series are from FOSI. The trends are calculated using running windows of the specified length. By construction, POP-MOVE and POP-MOVE-offset trend time series are identical, and only POP-MOVE is shown in (e). The simultaneous correlation coefficients are also listed for each panel between the given time series.

longer averaging lengths (Bretherton et al., 1999), the correlations are significant at 95% level up to about 4 years and at ~80% level for longer time scales. These findings seem to be consistent with those of Kanzow et al. (2008) who indicate that deep meridional fluctuations in the western basin on multi-annual time scales can be regarded as a useful approximation to the full-basin AMOC changes.

Vertical profiles of the zonally averaged meridional velocity for the internal transport component at MOVE are shown from observations and FOSI in Figure 2c. Changing the level-of-no-motion from 4,950 m (black solid line) to 1,200 m (black dotted line) in observations allows a northward AABW flow at depth without changing the shape of the profile. However, the mean transport decreases from 22.6 to 17.3 Sv over the full observational record. Such an adjustment of the internal component seems consistent with the model truth (POP-MOVE-vel; orange solid line) at depth, but the model does not show a level-of-no-motion at 1,200 m. Not surprisingly, the model profiles obtained via different methods differ from each other. While all capture the two southward transport maxima at ~4,000 and ~1,800 m evident in observations, their minimum in southward flow is located deeper at ~3,500 m, compared to ~3,000 m in observations. In general, the model meridional velocities are weaker than in observations. The zonal-mean reference velocity at 4,950 m from FOSI is clearly not zero, varying between ~1 and 4 mm s^{-1} (Figure 2d). Furthermore, it shows a rather rich variability on interannual-to-decadal time scales. This non-zero reference velocity largely reflects the northward transport associated with the AABW (Figure 2e) with the two time series correlated at 0.85. As also pointed out in FW18, very small variations in the reference velocities can translate into large volume transport differences across a section. For example, a difference of 1 mm s^{-1} in the reference velocity results in a transport difference of ~4 Sv across the MOVE site.

FOSI's relatively long record along with the availability of a model *truth* allows an assessment of how consistent transport trends are on various time scales between the RAPID and MOVE sites. Figures 3a–3c show the time series of the 5-year (pentadal), 10-year (decadal), and 30-year (multi-decadal) trends for the model truth, computed using running windows of the specified length. The simultaneous correlations of the

MOVE and RAPID trends monotonically increase as the trends are computed over longer periods with the 30-years trends essentially being identical at both sites with a correlation coefficient of 0.99. On pentadal and decadal time scales, some segments show comparable trends or variations at both sites, for example, during the 1970s for pentadal and between the mid-1970s to the mid-1980s for decadal. However, there are also several segments where the trends do not agree, for example, between 1995 and 2000 for pentadal and between 1990 and 1995 for decadal. The time scale and time segment dependence of agreements between MOVE and RAPID possibly depend on the processes responsible for coherence being dominant at both latitudes during certain time periods, with broader regional or basin-wide spatial scales. In contrast, local processes, such as wind forcing, may produce stronger variability at either one of the locations, breaking coherency (e.g., McCarthy et al., 2012; Srokosz & Bryden, 2015). Figures 3a–3c also include the corresponding trends from the compensating transport for RAPID from FOSI, showing that this transport can play a significant role in determining the trends of the total transport. Indeed, its trends are generally much larger than those of the total, dictating the sign of the latter during many periods, particularly on pentadal time scales.

The decadal model trends at the RAPID and MOVE locations from the transport methods are presented in Figures 3d and 3e, respectively. At RAPID, the observational method and the model truth trends agree well with a correlation coefficient of 0.93 (Figure 3d). At MOVE, the trends based on methods that include time-varying reference velocities match that of the model truth with correlation coefficients of 0.92 for POP-MOVE-ref and 0.96 for POP-MOVE-td. In contrast, the observational methods correlate relatively poorly with the model truth with correlations of 0.41 largely due to an offset in the variability of trends prior to ∼1995. Corresponding analysis of pentadal and multi-decadal trends produce qualitatively similar results (not shown).

For the 2004–2015 period analyzed in FW18, the FOSI trends are consistent for MOVE and RAPID and across the methods, all showing weakening transports at rates of −1.2 to −2.5 Sv decade^{-1} (Table S3). This consistency in trends is at odds with the observational estimates that show an increasing trend at MOVE (+8.1 Sv decade^{-1}) and a decreasing trend at RAPID (−3.7 Sv decade^{-1}) reported in FW18. (Smaller-than-observed trends appear to be common among models as discussed in Roberts et al. (2014)). FW18 attributes this discrepancy in observations to the compensating flow trend which reverses the sign of a strengthening (southward) internal transport component at RAPID which is otherwise consistent with the increasing transport at MOVE. In FOSI, the compensating transport magnitude is comparable to those of observations (−6.5 vs. ∼ −10 Sv in observations) for 2004–2015 (Figure S1). However, its trend of +0.25 Sv decade^{-1} during this period is rather small, though the compensating transport can certainly impact the trends during other periods. As discussed above, because the other transport components show very little interannual to decadal variability, variability of the compensating transport in FOSI primarily reflects that of the interior geostrophic transport, with the two time series negatively correlated (Figure S1). Specifically, when the southward geostrophic flow is large, it mostly balances the northward Florida Current component, with the compensating transport remaining relatively small. In contrast, when the southward geostrophic flow is small, the compensating transport becomes large to partially balance the Florida Current flow. Again, these results are consistent with those from the RAPID observations (Figure 12 of FW18).

4. Summary and Discussion

Reference level assumptions used to calculate AMOC transports at the RAPID and MOVE observing arrays are revisited in an eddying ocean model. In addition to the observational methods, several alternative transport calculations are also considered, focusing on the details of the reference levels, associated reference velocities, and transport trends on various time scales. At RAPID, the transports from the observational method and the model truth agree well. In contrast, there are significant differences among the estimates obtained with various methods for the MOVE site. Notably, the observational method and the model truth show important differences. The results also indicate that the MOVE-section transport estimates are good approximations for the total trans-basin AMOC transport particularly on pentadal and longer time scales.

The transport differences at MOVE are due to differences in the reference velocities used in the respective calculations. Specifically, the model solutions show relatively large and time-varying meridional velocities at 4,950-m depth associated with the northward flowing AABW, and thus, they do not support a

level-of-no-motion at this depth on either short or long time scales considered here. The methods that employ time-varying reference velocities produce transports that are the closest to the model truth. Transport differences of order 10 Sv or even larger are also seen on annual time scales between the observational estimates at MOVE that use zero and nonzero reference velocities at depth, but the record lengths are rather short (Figure 13 of FW18).

At the RAPID site, the model solutions also have time-varying meridional velocities at 4,820-m depth (~4,820 dbar), but with significantly smaller amplitudes than at MOVE (not shown). The RAPID mass balance term compensates for changes in the reference velocity there. Good agreement between the model truth and the RAPID model equivalent suggests that the removal of a hypsometric, time-varying barotropic compensation transport is an effective way to address the issues associated with the barotropic or external component of the geostrophic transport. However, the compensation term determines the sign of the decadal trend in the observations (FW18). While the approach is apparently justified by the model solutions shown here, it is of utmost importance to identify and apply appropriate methods to treat reference velocities in large-scale applications of geostrophic balance.

In stark contrast with observations, the model transport trends at MOVE and RAPID agree with each other for 2004–2015, both showing slight declines. However, with large interannual changes at both sites, it is difficult to attach much significance to such short-term trends. On centennial time scales, an analysis of the CESM2 historical and future scenario simulations indicates that the model MOVE and RAPID transports have largely consistent trends (not shown).

Our study reiterates the known challenges associated with treatments of reference velocities in observational transport estimates, that are not unique to the two sites considered. There is an urgent need to address these issues so that the observational methods can be used not only to evaluate latitudinal consistency of AMOC characteristics in observations but also in the analysis of model simulations of future AMOC changes. Recent efforts combining the GRACE satellite data sets with in situ data from moorings and repeat hydrography can provide much-needed reliable estimates of deep ocean transport variability via bottom pressure estimates (Koelling et al., 2020; see also Text S2). Our results also suggest that altimetry could potentially provide another solution for estimating time-varying reference velocities required by the end-point geostrophic arrays.

Acknowledgments
This work is supported by the grant NA18OAR4310429 from the National Oceanic and Atmospheric Administration (NOAA), Climate Program Office (CPO), Climate Variability and Predictability Program; Modeling Analysis, Predictions, and Projections Program; and the NOAA Global Ocean Monitoring and Observing (GOMO) Program, and by the Department of Energy, Earth and Environmental System Modeling, Regional and Global Model Analysis Program. The CESM project is supported primarily by the National Science Foundation (NSF). This material is also based upon work supported by the National Center for Atmospheric Research (NCAR), which is a major facility sponsored by the NSF under Cooperative Agreement No. 1852977. The high-resolution CESM2 FOSI simulation was performed on the HPC systems at the Texas Advanced Computing Center by the International Laboratory for High-Resolution Earth System Prediction (iHESP). RAPID is funded by the UK Natural Environment Research Council for the RAPID-AMOC program, NSF (grant no. 1332978), and NOAA CPO (grant no. 100007298). MOVE is supported by the NOAA GOMO Program under grant NA20OAR4320278. We thank two anonymous reviewers for their constructive comments and suggestions.

Data Availability Statement

The MOVE and RAPID observational data sets are available at http://mooring.ucsd.edu/dev/move/ and https://www.rapid.ac.uk/rapidmoc/, respectively. The METRIC package is available at https://doi.org/10.5281/zenodo.4708277. CESM versions are freely available at www.cesm.ucar.edu:/models/cesm2/. The data sets from the METRIC package which are based on the CESM2 high-resolution FOSI simulations are available from the NCAR Digital Asset Services Hub (DASH) at https://doi.org/10.5065/zrr4-e320.

References

Bower, A., Lozier, S., Biastoch, A., Drouin, K., Foukal, N., Furey, H., et al. (2019). Lagrangian views of the pathways of the Atlantic meridional overturning circulation. *Journal of Geophysical Research: Oceans*, *124*, 5313–5335. https://doi.org/10.1029/2019JC015014

Bretherton, C. S., Widmann, M., Dymnikov, V. P., Wallace, J. M., & Bladé, I. (1999). The effective number of spatial degrees of freedom of a time-varying field. *Journal of Climate*, *12*, 1990–2009. https://doi.org/10.1175/1520-0442(1999)012<1990:tenosd>2.0.co;2

Bryden, H. L., Longworth, H. R., & Cunningham, S. A. (2005). Slowing of the Atlantic meridional overturning circulation at 25° N. *Nature*, *438*, 655–657. https://doi.org/10.1038/nature04385

Buckley, M. W., & Marshall, J. (2016). Observations, inferences, and mechanisms of the Atlantic meridional overturning circulation: A review. *Reviews of Geophysics*, *54*, 5–63. https://doi.org/10.1002/2015RG000493

Chang, P., Zhang, S., Danabasoglu, G., Yeager, S. G., Fu, H., Wang, H., et al. (2020). An unprecedented set of high-resolution earth system simulations for understanding multiscale interactions in climate variability and change. *Journal of Advances in Modeling Earth Systems*, *12*, e2020MS002298. https://doi.org/10.1029/2020MS002298

Chassignet, E. P., Yeager, S. G., Fox-Kemper, B., Bozec, A., Castruccio, F., Danabasoglu, G., et al. (2020). Impact of horizontal resolution on global ocean-sea ice model simulations based on the experimental protocols of the Ocean Model Intercomparison Project phase 2 (OMIP-2). *Geoscientific Model Development*, *13*, 4595–4637. https://doi.org/10.5194/gmd-13-4595-2020

Cunningham, S. A., Kanzow, T., Rayner, D., Baringer, M. O., Johns, W. E., Marotzke, J., et al. (2007). Temporal variability of the Atlantic meridional overturning circulation at 26.5°N. *Science*, *317*, 935–938. https://doi.org/10.1126/science.1141304

Danabasoglu, G., Andres, M., Buckley, M., Donohue, K., Hu, A., Little, C., et al. (2018). 2018 US AMOC Science Team report on progress and priorities. *A US CLIVAR Report*, *2018–2*, 156. https://doi.org/10.5065/D6FQ9VDB

Danabasoglu, G., Bates, S. C., Briegleb, B. P., Jayne, S. R., Jochum, M., Large, W. G., et al. (2012). The CCSM4 ocean component. *Journal of Climate*, *25*, 1361–1389. https://doi.org/10.1175/JCLI-D-11-00091.1

Danabasoglu, G., Lamarque, J.-F., Bacmeister, J., Bailey, D. A., DuVivier, A. K., Edwards, J., et al. (2020). The Community Earth System Model version 2 (CESM2). *Journal of Advances in Modeling Earth Systems*, *12*, e2019MS001916. https://doi.org/10.1029/2019MS001916

Danabasoglu, G., Yeager, S. G., Bailey, D., Behrens, E., Bentsen, M., Bi, D., et al. (2014). North Atlantic simulations in Coordinated Ocean-ice Reference Experiments phase II (CORE-II). Part I: Mean states. *Ocean Modelling*, *73*, 76–107. https://doi.org/10.1016/j.ocemod.2013.10.005

Danabasoglu, G., Yeager, S. G., Kim, W. M., Behrens, E., Bentsen, M., Bi, D., et al. (2016). North Atlantic simulations in Coordinated Ocean-ice Reference Experiments phase II (CORE-II). Part II: Inter-annual to decadal variability. *Ocean Modelling*, *97*, 65–90. https://doi.org/10.1016/j.ocemod.2015.11.007

Frajka-Williams, E., Ansorge, I. J., Baehr, J., Bryden, H. L., Chidichimo, M. P., Cunningham, S. A., et al. (2019). Atlantic meridional overturning circulation: Observed transport and variability. *Frontiers in Marine Sciences*, *6*. UNSP 260. https://doi.org/10.3389/fmars.2019.00260

Frajka-Williams, E., Lankhorst, M., Koelling, J., & Send, U. (2018). Coherent circulation changes in the deep North Atlantic from 16°N and 26°N transport arrays. *Journal of Geophysical Research*, *123*, 3427–3443. https://doi.org/10.1029/2018JC013949

Hirschi, J., Baehr, J., Marotzke, J., Stark, J., Cunningham, S., & Beismann, J.-O. (2003). A monitoring design for the Atlantic meridional overturning circulation. *Geophysical Research Letters*, *30*, 1413. https://doi.org/10.1029/2002GL016776

Kanzow, T., Send, U., & McCartney, M. (2008). On the variability of the deep meridional transports in the tropical North Atlantic. *Deep Sea Research Part I: Oceanographic Research Papers*, *55*, 1601–1623. https://doi.org/10.1016/j.dsr.2008.07.011

Kanzow, T., Send, U., Zenk, W., Chave, A. D., & Rhein, M. (2006). Monitoring the integrated deep meridional flow in the tropical North Atlantic: Long-term performance of a geostrophic array. *Deep Sea Research Part I: Oceanographic Research Papers*, *53*, 528–546. https://doi.org/10.1016/j.dsr.2005.12.007

Koelling, J., Send, U., & Lankhorst, M. (2020). Decadal strengthening of interior flow of North Atlantic Deep Water observed by GRACE satellites. *Journal of Geophysical Research: Oceans*, *125*, e2020JC016217. https://doi.org/10.1029/2020JC016217

Larsen, J. C., & Sanford, T. B. (1985). Florida current volume transports from voltage measurements. *Science*, *227*, 302–304. https://doi.org/10.1126/science.227.4684.302

Li, F., Lozier, M. S., & Johns, W. E. (2017). Calculating the meridional volume, heat, and freshwater transports from an observing system in the subpolar North Atlantic: Observing system simulation experiment. *Journal of Atmospheric and Oceanic Technology*, *34*, 1483–1500. https://doi.org/10.1175/JTECH-D-16-0247.1

Lozier, M. S., Li, F., Bacon, S., Bahr, F., Bower, A. S., Cunningham, S. A., et al. (2019). A sea change in our view of overturning in the subpolar North Atlantic. *Science*, *363*, 516–521. https://doi.org/10.1126/science.aau6592

McCarthy, G., Frajka-Williams, E., Johns, W. E., Baringer, M. O., Meinen, C. S., Bryden, H. L., et al. (2012). Observed interannual variability of the Atlantic meridional overturning circulation at 26.5°N. *Geophysical Research Letters*, *39*, L19609. https://doi.org/10.1029/2012GL052933

McCarthy, G. D., Brown, P. J., Flagg, C. N., Goni, G., Houpert, L., Hughes, C. W., et al. (2020). Sustainable observations of the AMOC: Methodology and technology. *Reviews of Geophysics*, *58*, e2019RG000654. https://doi.org/10.1029/2019RG000654

McCarthy, G. D., Smeed, D. A., Johns, W. E., Frajka-Williams, E., Moat, B. I., Rayner, D., et al. (2015). Measuring the Atlantic meridional overturning circulation at 26°N. *Progress in Oceanography*, *130*, 91–111. https://doi.org/10.1016/j.pocean.2014.10.006

Meinen, C. S., Baringer, M. O., & Garcia, R. F. (2010). Florida current transport variability: An analysis of annual and longer-period signals. *Deep Sea Research Part I: Oceanographic Research Papers*, *57*, 835–846. https://doi.org/10.1016/j.dsr.2010.04.001

Meinen, C. S., Speich, S., Piola, A. R., Ansorge, I., Campos, E., Kersalé, M., et al. (2018). Meridional overturning circulation transport variability at 34.5°S during 2009-2017: Baroclinic and barotropic flows and the dueling influence of the boundaries. *Geophysical Research Letters*, *45*, 4180–4188. https://doi.org/10.1029/2018GL077408

Perez, R. C., Garzoli, S. L., Meinen, C. S., & Matano, R. P. (2011). Geostrophic velocity measurement techniques for the meridional overturning circulation and meridional heat transport in the South Atlantic. *Journal of Atmospheric and Oceanic Technology*, *28*, 1504–1521. https://doi.org/10.1175/JTECH-D-11-00058.1

Roberts, C. D., Jackson, L., & McNeall, D. (2014). Is the 2004-2012 reduction of the Atlantic meridional overturning circulation significant? *Geophysical Research Letters*, *41*, 3204–3210. https://doi.org/10.1002/2014GL059473

Roberts, C. D., Waters, J., Peterson, K. A., Palmer, M. D., McCarthy, G. D., Frajka-Williams, E., et al. (2013). Atmosphere drives recent interannual variability of the Atlantic meridional overturning circulation at 26.5°N. *Geophysical Research Letters*, *40*, 5164–5170. https://doi.org/10.1002/grl.50930

Sanford, T. B. (1982). Temperature transport and motional induction in the Florida Current. *Journal of Marine Research*, *40*(Suppl), 621–639.

Send, U., Lankhorst, M., & Kanzow, T. (2011). Observation of decadal change in the Atlantic meridional overturning circulation using 10 years of continuous transport data. *Geophysical Research Letters*, *38*, 24606. https://doi.org/10.1029/2011GL049801

Sinha, B., Smeed, D. A., McCarthy, G., Moat, B. I., Josey, S. A., Hirschi, J. J.-M., et al. (2018). The accuracy of estimates of the overturning circulation from basin-wide mooring arrays. *Progress in Oceanography*, *160*, 101–123. https://doi.org/10.1016/j.pocean.2017.12.001

Smeed, D. A., Josey, S. A., Beaulieu, C., Johns, W. E., Moat, B. I., Frajka-Williams, E., et al. (2018). The North Atlantic Ocean is in a state of reduced overturning. *Geophysical Research Letters*, *45*, 1527–1533. https://doi.org/10.1002/2017GL076350

Smeed, D. A., McCarthy, G. D., Cunningham, S. A., Frajka-Williams, E., Rayner, D., Johns, W. E., et al. (2014). Observed decline of the Atlantic meridional overturning circulation 2004-2012. *Ocean Science*, *10*, 29–38. https://doi.org/10.5194/os-10-29-2014

Smith, R., Jones, P., Briegleb, B., Bryan, F., Danabasoglu, G., Dennis, J., et al. (2010). *The Parallel Ocean Program (POP) reference manual, ocean component of the Community Climate System Model (CCSM)* (LANL Tech. Report, LAUR-10-01853, p. 141).

Srokosz, M. A., & Bryden, H. L. (2015). Observing the Atlantic meridional overturning circulation yields a decade of inevitable surprises. *Science*, *348*, 1255575. https://doi.org/10.1126/science.1255575

Stepanov, V. N., Iovino, D., Masina, S., Storto, A., & Cipollone, A. (2016). Methods of calculation of the Atlantic meridional heat and volume transports from ocean models at 26.5°N. *Journal of Geophysical Research: Oceans*, *121*, 1459–1475. https://doi.org/10.1002/2015JC011007

Sutton, R. T., McCarthy, G. D., Robson, J., Sinha, B., Archibald, A. T., & Gray, L. J. (2018). Atlantic multidecadal variability and the U.K. ACSIS program. *Bulletin of the American Meteorological Society*, *99*, 415–425. https://doi.org/10.1175/BAMS-D-16-0266.1

Toole, J. M., Andres, M., Le Bras, I. A., Joyce, T. M., & McCartney, M. S. (2017). Moored observations of the deep western boundary current in the NW Atlantic: 2004-2014. *Journal of Geophysical Research: Oceans*, *122*, 7488–7505. https://doi.org/10.1002/2017JC012984

Toole, J. M., Curry, R. G., Joyce, T. M., McCartney, M., & Peña-Molino, B. (2011). Transport of the North Atlantic deep western boundary current about 39°N, 70°W: 2004-2008. *Deep Sea Research Part II: Topical Studies in Oceanography*, *58*, 1768–1780. https://doi.org/10.1016/j.dsr2.2010.10.058

Tsujino, H., Urakawa, L. S., Griffies, S. M., Danabasoglu, G., Adcroft, A. J., Amaral, A. E., et al. (2020). Evaluation of global ocean-sea-ice model simulations based on the experimental protocols of the Ocean Model Intercomparison Project phase 2 (OMIP-2). *Geoscientific Model Development*, *13*, 3643–3708. https://doi.org/10.5194/gmd-13-3643-2020

Tsujino, H., Urakawa, S., Nakano, H., Small, R. J., Kim, W. M., Yeager, S. G., et al. (2018). JRA-55 based surface dataset for driving ocean-sea-ice models (JRA55-do). *Ocean Modelling*, *130*, 79–139. https://doi.org/10.1016/j.ocemod.2018.07.002

Zhang, R., Sutton, R., Danabasoglu, G., Kwon, Y.-O., Marsh, R., Yeager, S. G., et al. (2019). A review of the role of the Atlantic meridional overturning circulation in Atlantic multidecadal variability and associated climate impacts. *Reviews of Geophysics*, *57*, 316–375. https://doi.org/10.1029/2019RG000644

References From the Supporting Information

Jackett, D. R., & McDougall, T. J. (1995). Minimal adjustment of hydrographic profiles to achieve static stability. *Journal of Atmospheric and Oceanic Technology*, *12*, 381–389. https://doi.org/10.1175/1520-0426(1995)012<0381:MAOHPT>2.0.CO;2

Roberts, C. D. (2017). *cdr30/RapidMoc: RapidMoc v1.0.1 (Version v1.0.1)*. Zenodo. https://doi.org/10.5281/zenodo.1036387